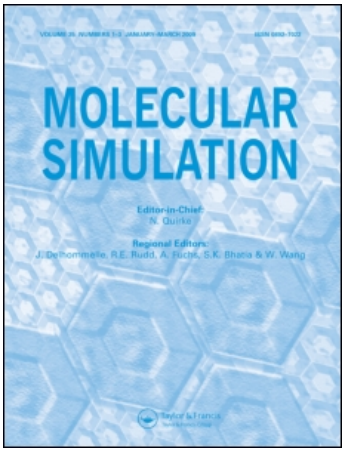

Molecular Simulation
Publication details, including instructions for authors and subscription information:
http://www.informaworld.com/smpp/title~content=t713644482

Molecular simulation of cage occupancy and selectivity of binary THF-H_2 sII hydrate

Dong-Hyuk Chun[a]; Tai-Yong Lee[a]
[a] Department of Chemical and Biomolecular Engineering, Korea Advanced Institute of Science and Technology, Daejeon, South Korea

To cite this Article Chun, Dong-Hyuk and Lee, Tai-Yong(2008) 'Molecular simulation of cage occupancy and selectivity of binary THF-H_2 sII hydrate', Molecular Simulation, 34: 9, 837 — 844
To link to this Article: DOI: 10.1080/08927020802301946
URL: http://dx.doi.org/10.1080/08927020802301946

Molecular Simulation
Vol. 34, No. 9, August 2008, 837–844

Taylor & Francis
Taylor & Francis Group

Molecular simulation of cage occupancy and selectivity of binary THF–H_2 sII hydrate

Dong-Hyuk Chun[1] and Tai-Yong Lee*

Department of Chemical and Biomolecular Engineering, Korea Advanced Institute of Science and Technology, Daejeon, South Korea

(*Received 19 June 2008; final version received 25 June 2008*)

The hydrogen capacity of the binary THF–H_2 sII hydrate is determined by the cage occupancy and by the selectivity of guest molecules. Grand canonical Monte Carlo (GCMC) simulation is used to study the cage occupancy and selectivity of guest molecules from the equilibrium configuration of the binary sII hydrate. The cage framework is regarded as a rigid body and the number of guest molecules is varied to preserve the grand canonical ensemble. The occupancy and selectivity were investigated at a temperature of 270 K for pressures ranging from 0.1 to 200 MPa. It was found that most large cages select THF as guest molecules while small cages include only hydrogen molecules. Multiple occupancy of hydrogen, up to four molecules in large cages and two molecules in small cages, was found as the pressure increases. GCMC results show that the hydrogen capacity is approximately 1.1 wt% at 200 MPa.

Keywords: binary sII hydrate; hydrogen; tetrahydrofuran; cage occupancy; selectivity; GCMC

1. Introduction

Clathrate hydrate denotes a class of solid compounds which consist of water and guest molecules. Water molecules make up the host cage structure from hydrogen bonds, and the clathrate constructed by cages is stabilised by the inclusion of guest molecules such as low molecular weight gases or volatile liquids. This can contain a large amount of gas and can be separated easily into water and guest molecules as these molecules are combined via physical rather than chemical bonds. For these reasons, clathrate hydrate has been proposed as a storage medium for a variety of gases.

Mao et al. [1] demonstrated multiple occupancies of sII hydrogen hydrates in 2002. They suggested that two hydrogen molecules and four hydrogen molecules could enter small cages and large cages, respectively, in which sII hydrates were theoretically able to store 5 wt% of hydrogen. The possibility of sII hydrates for hydrogen storage has been studied since [2–6]. However, it is difficult for sII hydrates to be used commercially for hydrogen storage, as pure hydrogen hydrates are formed at an extreme pressure typically greater than 200 MPa. Lee et al. [7], in 2005, offered a new synthesizing method for sII hydrates that was able to decrease the formation pressure through the use of tetrahydrofuran (THF) in the hydrate formation process. Their results suggested that binary THF–H_2 sII hydrates can be formed at modest pressure and that they are able to store up to 4 wt% of hydrogen at 12 MPa by tuning the amount of THF. There have been successive studies to support these results, such as molecular dynamics simulation [8] or the van der Waals and Platteeuw (vdWP) theory [9] for THF–H_2 binary hydrates. However, experiments using high resolution neutron diffraction [10] only showed single occupancy in small cages of binary hydrates at a formation pressure of 70 MPa. Similar results were reported by experiments using gas release measurements [11]. The hydrogen capacity of binary sII hydrates remains in dispute.

In this work, Monte Carlo simulations are performed under a grand-canonical ensemble to study the hydrogen capacity as determined by the cage occupancy and the selectivity of guest molecules. Grand-canonical Monte Carlo (GCMC) simulation is a representative method that is widely used for adsorption problems. It allows consideration of the formation of sII hydrate as adsorption phenomena. Hence, guest molecules are regarded as adsorbates and water cages are regarded as adsorbents. The equilibrium state is obtained from GCMC at 270 K under pressure variances, and cage occupancy and selectivity are studied using an equilibrium configuration. Molecular models and the GCMC methods as applied here are explained in the next section in detail.

2. Molecular simulations

2.1 *Molecular models and interaction energy*

Molecular simulations were performed for sII clathrate hydrates. The simulation system consisted of eight unit cells of the sII hydrate, which each unit cell consisting of H_2O, THF and H_2 molecules. Initially, oxygen atoms in water molecules were located at the *Fd3m* cubic structure. The size and structural configuration of the sII hydrate were determined by data proposed by Mak and McMullan [12].

*Corresponding author. Email: tylee@kaist.ac.kr

ISSN 0892-7022 print/ISSN 1029-0435 online

DOI: 10.1080/08927020802301946
http://www.informaworld.com

The cage structure of the sII hydrate was obtained after several million of Monte Carlo iterations. The cage framework connected by hydrogen bonds between water molecules formed through the rotating and displacing activities of the Monte Carlo simulation. The configuration of the guest molecules was determined via GCMC on the assumption that the cage framework has a rigid body. This assumption is feasible given that the hydrogen bonding strength, which forms a cage framework, is much larger compared to the van der Waals bonding strength between the guest molecule and the host molecules forming the cage framework. The intermolecular interaction energy was calculated using the Lennard-Jones potential for van der Waals interactions and the Coulombic potential for electrostatic interactions. The interaction energy between two component, i and j, is given by

$$U_{ij} = \sum_{l\in i}\sum_{m\in j}\frac{q_{il}q_{jm}}{4\pi\varepsilon_o r_{il\,jm}} + 4\varepsilon_{ij}\left[\left(\frac{\sigma_{ij}}{r_{ij}}\right)^{12} - \left(\frac{\sigma_{ij}}{r_{ij}}\right)^{6}\right], \quad (1)$$

where q_{il} is the charge of atom l in molecule i, ε_o is the vacuum permittivity, r_{ij} is the distance between sites i and j, and ε_{ij} and σ_{ij} are the Lennard-Jones parameters. Every molecule used in the simulation is regarded as a rigid body, as intramolecular interactions are not important in the current work.

The interaction parameters of water are referred to an extended simple point-charge (SPC/E) model. Water molecules have three-site partial charges located directly on the oxygen and hydrogen atoms in the SPC/E model [13]. Hydrogen molecules are considered to have three-site partial charges located on the hydrogen atoms and the centre of mass so that the point-charges are calculated accurately. Silvera–Goldman interaction parameters [8] are used for hydrogen. The interaction parameters and the geometry of water and hydrogen are shown in Table 1. The twist form of THF, known as the most stable form, is used in the simulation. Using the Gaussian 03 program suite [14], the structure of THF was optimised and the electrostatic interaction parameters were obtained [8]. The van der Waals interaction parameters were obtained from the general AMBER force field [15]. The interaction parameters and geometry of THF are shown in Table 2.

Long-range interaction of the electrostatic term, U_{RF}, was corrected by adding a reaction field term [16] and expressed by following equation:

$$U_{\mathrm{RF}} = \frac{q_{il}q_{jm}}{4\pi\varepsilon_o}\frac{\varepsilon_{\mathrm{RF}}-1}{2\varepsilon_{\mathrm{RF}}+1}\frac{r_{ij}^2}{r_{\mathrm{cutoff}}^3}, \quad (2)$$

where $\varepsilon_{\mathrm{RF}}$ is a prior estimate of the static dielectric constant and r_{cutoff} is the cut-off distance. The Lorentz–Berthelot

Table 1. Interaction parameters and structure of water and hydrogen utilised in the GCMC simulations.

Molecule	Atom	q (e)	σ (nm)	ε (kJ/mol)	Geometry
Water	O	−0.8476	0.3166	0.6502	O—H = 1.0 A
	H	0.4238	–	0	H—O—H = 109.47°
Hydrogen	HCM	−0.9864	0.3038	0.2852	H—H = 0.7414 A
	H	0.4932	–	0	

Note: The SPC/E potential model [13] is used for water and the Silvera–Goldman interaction parameters [8] are used for hydrogen.

Table 2. Interaction parameters and coordinates of THF utilised in the GCMC simulations.

				Coordinates (A)		
Atom	q (e)	σ (nm)	ε (kJ/mol)	x	y	z
O	−0.492219	0.3	0.7113	0	0	0
C1	0.259687	0.34	0.4577	1.169407	0.825076	−0.12281
C2	−0.006023	0.34	0.4577	0.729561	2.250276	0.228417
C3	−0.01543	0.34	0.4577	−0.738753	2.245646	−0.22141
C4	0.274293	0.34	0.4577	−1.170072	0.82076	0.13871
H1	−0.011396	0.2471	0.0657	1.942039	0.433969	0.544202
H2	−0.006238	0.2471	0.0657	1.541117	0.766226	−1.15392
H3	−0.01616	0.2645	0.0657	1.333678	3.010977	−0.27008
H4	0.025872	0.2645	0.0657	0.796043	2.41653	1.307841
H5	0.027908	0.2645	0.0657	−0.806626	2.404382	−1.30189
H6	−0.015166	0.2645	0.0657	−1.346254	3.006443	0.272869
H7	−0.014974	0.2471	0.0657	−1.950003	0.42455	−0.51644
H8	−0.010155	0.2471	0.0657	−1.527741	0.764462	1.175202

Note: The structure and electrostatic interaction parameters of THF are obtained from Gaussian 03 [14] and the Lennard-Jones potential parameters are obtained from the general AMBER force field [15].

mixing rule [17] is used for the interaction between two molecules and expressed by following equation:

$$\sigma_{12} = \frac{\sigma_1 + \sigma_2}{2}, \quad \varepsilon_{12} = \sqrt{\varepsilon_1 \varepsilon_2}. \tag{3}$$

2.2 Calculation of chemical potentials for guest molecules

The chemical potential is the most important parameter in GCMC simulation. A precise value of the chemical potential gives the accurate results about cage occupancy and selectivity. The chemical potential can be obtained via the distribution-function theory of equilibrium fluids. In this theory, there are three basic assumptions [18]: classical statistical mechanics can be used for the translational partition function; the interamolecular interactions are independent of the intermolecular interactions; and intermolecular potentials are pairwise additive, that is,

$$U = \sum_i \sum_j \phi(r_{ij}), \tag{4}$$

where ϕ is a pair-potential energy function. The aforementioned assumptions are applicable to the current simulation system. In distribution-function theory, the equation of state under these assumptions is expressed by

$$PV = Nk_BT - \frac{2\pi}{3}\frac{N^2}{V}\int_0^\infty \frac{d\phi}{dr} g(r) r^3 dr, \tag{5}$$

where k_B is a Boltzmann constant and $g(r)$ is a radial distribution function. The residual chemical potential is written as

$$\mu^r = \frac{2\pi}{3}\left\{\frac{\partial}{\partial N}\left[N^2 \int_\infty^V \frac{dV'}{V'^2}\int_0^\infty \frac{d\phi}{dr} g(r) r^3 dr\right]\right\}_{T,V}. \tag{6}$$

Finally, the chemical potential can be represented by [19],

$$\mu = k_BT\left[\ln\rho\left(\frac{h^2}{2\pi m k_BT}\right)^{\frac{3}{2}} - 1\right] + \int_0^\rho \left(P - \rho' k_BT\right)\frac{d\rho'}{\rho'^2} + \frac{P}{\rho}, \tag{7}$$

where m is the mass, h denotes Plank's constant and ρ is the number density ($= N/V$). The first term of Equation (7) is the ideal chemical potential and the following terms are the residual chemical potential obtained from Equations (5) and (6). The densities of hydrogen and THF are obtained for various pressures using isothermal–isobaric MC. The chemical potentials of hydrogen and THF are calculated by means of numerical integration with the relationship between the pressure and the density from Equation (7).

2.3 Monte Carlo simulation of the sII hydrate cage occupancy for multi-component guest molecules

The chemical potential, temperature and volume were fixed in GCMC method. In an equilibrium state, the chemical potentials of guest molecules are identical to those of their bulk fluid. Therefore, the number of adsorbates is changed to maintain the chemical potential of the bulk fluid which is determined at a given temperature and pressure. The conventional GCMC method has three types of moves: displacement, insertion and deletion. The related acceptance probabilities are as follows:

$$A(r \to r') = \exp\left[-\frac{(U(r') - U(r))}{k_BT}\right], \tag{8}$$

$$A(N \to N+1) = \frac{V}{\Lambda^3(N+1)}\exp\left[\frac{[\mu - (U_{N+1} - U_N)]}{k_BT}\right], \tag{9}$$

$$A(N \to N-1) = \frac{\Lambda^3 N}{V}\exp\left[-\frac{[\mu + (U_{N-1} - U_N)]}{k_BT}\right]. \tag{10}$$

Here, Λ is the thermal de Broglie wavelength. The current system has two types of guest molecules, THF and H_2. In the case of an adsorbing mixture, an additional type of move is used for the efficiency of the calculations. It is an exchange term and its acceptance probability is determined by [20]

$$A(i \to j) = \frac{\Lambda_i^3}{\Lambda_j^3}\frac{N_i}{N_j + 1}\exp\left[\frac{[\mu_j - \mu_i - (U_j - U_i)]}{k_BT}\right]. \tag{11}$$

Through the iterative GCMC moves introduced above, the sII hydrate system could achieve an equilibrium state.

The number of guest molecules (H_2 and THF) is controlled by insertions and deletions. In the conventional GCMC method, insertions of molecules are uniformly attempted in the entire system. However, the spaces of a cage framework are fixed in the system, so the acceptance probabilities of insertions decrease remarkably due to these

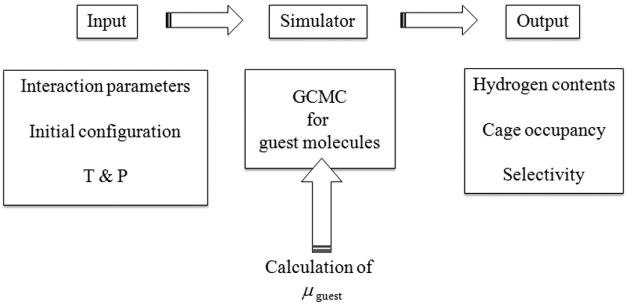

Figure 1. Simulation overview. GCMC is carried out with input variables and the chemical potentials of the guest molecules. Equilibrium states obtained from the GCMC describe the cage occupancy and selectivity of the guest molecules.

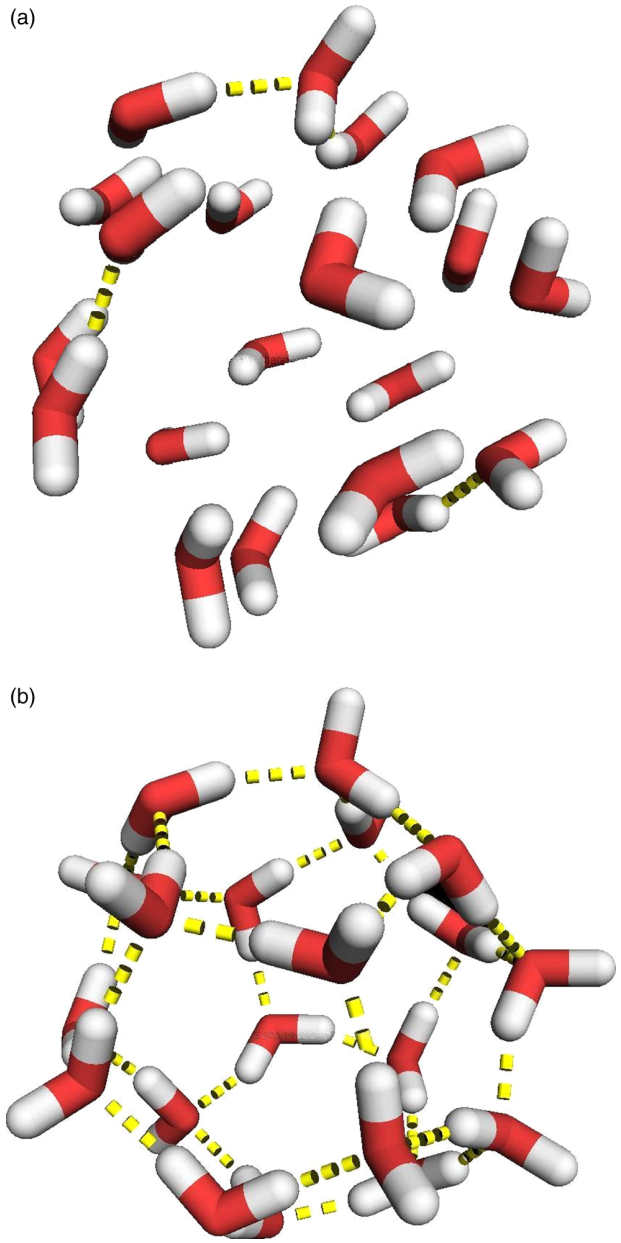

Figure 2. Formation of a small cage: (a) initial configuration of water molecules; (b) cage structure formed by the hydrogen-bonded water network. Water molecules randomly oriented form a cage framework through Monte Carlo simulation. Dashed lines denote the hydrogen bonds between water molecules.

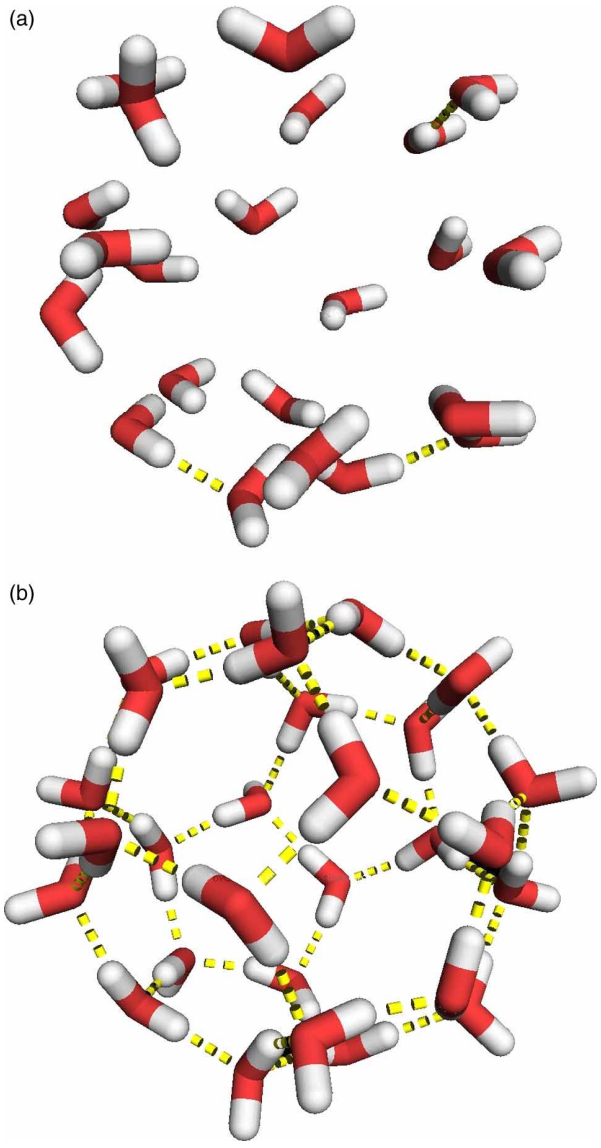

Figure 3. Formation of a large cage: (a) initial configuration of water molecules; (b) cage structure formed by the hydrogen-bonded water network.

inaccessible spaces. To improve the efficiency of the GCMC simulation, a biased GCMC technique was applied in the present simulation [21]. In this method, the total volume was substituted for the accessible volume, V_{acc}. To calculate V_{acc}, the total volume was discretised into elementary volumes and a guest molecule was placed at the centre of each elementary volume. The interaction energy between a guest molecule and a cage framework was then calculated. The elementary volume, which has interaction energy lower than $10^5 k_B$ in this work, was selected as a member of the accessible volume. Two values of V_{acc} should be calculated for H_2 and THF in the simulation. Insertions of guest molecules are only attempted at the centre of selected elementary volumes, and the acceptance probabilities for insertions and deletions are modified by replacing V with V_{acc}.

The simulation procedure followed the order illustrated in Figure 1. Interaction parameters, initial configurations, temperature and the pressure are given in the input step. GCMC simulation was carried out for guest molecules with the chemical potentials calculated and variables inputted. Finally, the cage occupancy and selectivity of the guest molecules were determined from

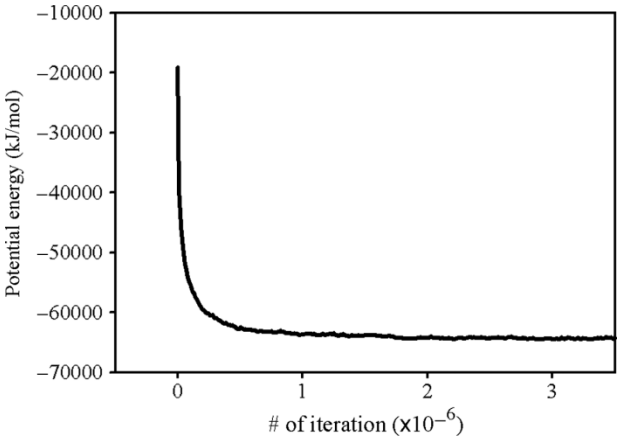

Figure 4. Change in the potential energy while the cage structure is constructed. The potential energy decreases as the water molecules form cage structures with hydrogen bonds.

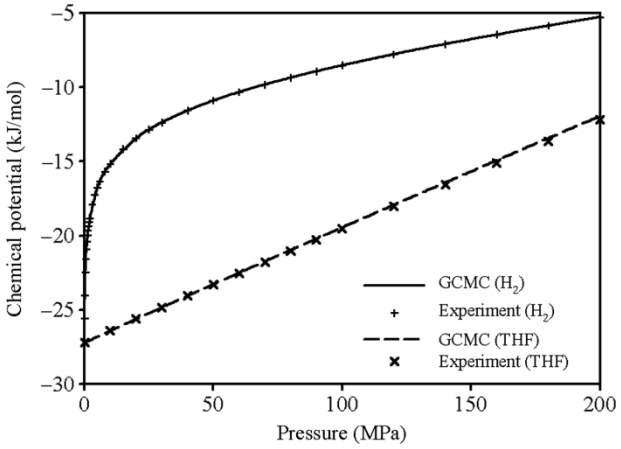

Figure 5. Chemical potentials of guest molecules. The solid line and the + symbols denote the chemical potentials of hydrogen. The dashed line and the × symbols denote the chemical potentials of THF. The chemical potential of each guest molecule is calculated from the Equation (7) with PVT data obtained from the GCMC simulations and experiments.

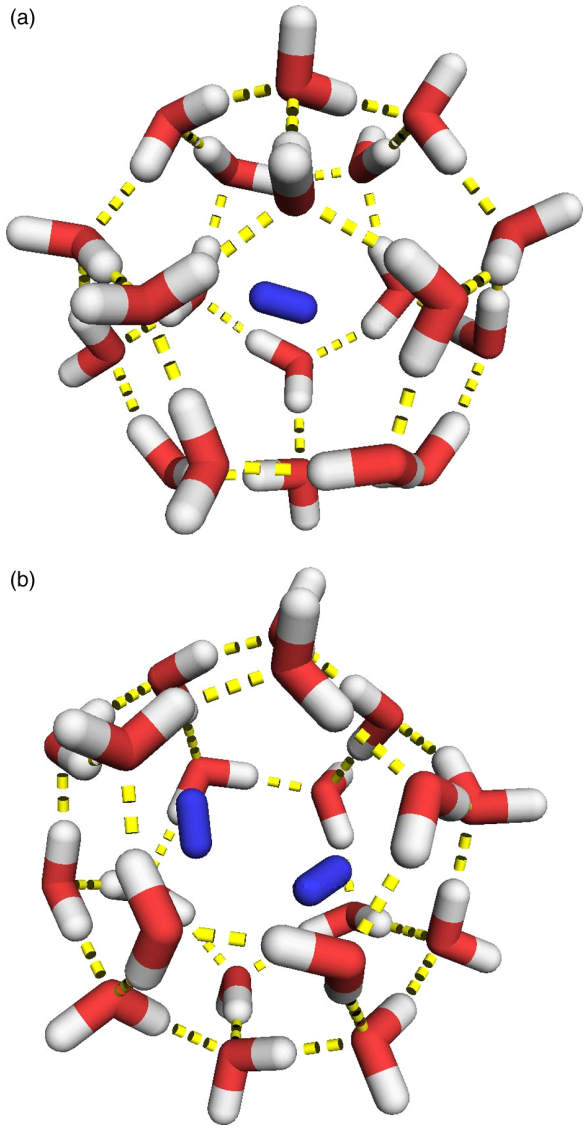

Figure 6. The configuration of hydrogen molecules in a small cage: (a) single occupancy of hydrogen in a small cage; (b) double occupancy of hydrogen in a small cage. The snapshots are obtained from GCMC simulation. The hydrogen molecules are located in the cage.

the equilibrium configuration of the binary sII hydrates obtained through the GCMC simulations.

Periodic boundary conditions were used to imitate an infinite number of molecules and to remove surface effects. Neighbour lists were created in order to reduce the computational load. They were updated at the interval of an appropriate iteration span.

3. Results and discussion

The cage structure of sII hydrate was obtained via the displacing and rotating moves in the Monte Carlo simulation. Water molecules initially positioned at *Fd3m* structure points with random directions (Figures 2(a) and 3(a)) were formed into cage structure with hydrogen bonds (Figures 2(b) and 3(b)). The potential energy converged on a stable value as the hydrogen bonds between the water molecules formed during the simulation. The change in the potential energy is shown in Figure 4.

The relationship between the pressures and densities of pure guest molecules were obtained by isothermal–isobaric MC, and the chemical potentials were calculated using Equation (7). Figure 5 shows that the chemical potentials calculated from the simulation data are remarkably consistent with those calculated from experimental PVT data [22,23].

GCMC simulations were carried out at T = 270 K at pressures ranging from 0.1 to 200 MPa with the rigid cage framework and the chemical potentials of the guest molecules. The equilibrium state of the guest molecules was obtained at given temperature and pressures. The cage occupancy and selectivity of the guest molecules were obtained from the configuration of the guest molecules at an equilibrium state. Figures 6 and 7, respectively, illustrate the observed forms of hydrogen molecules in small and large cages through simulation.

The cage occupancy obtained via GCMC was compared with the Langmuir adsorption isotherm [11] in the vdWP theory, as expressed by the following equation:

$$\theta_{ji} = \frac{C_{ji}(T) f_i(T,P)}{1 + \sum_k C_{jk}(T) f_k(T,P)}. \tag{12}$$

In this equation, f_i is the fugacity of component i, and C_{ji} is the Langmuir constant of component i in cage j. The Langmuir constant is expressed by

$$C_{ji}(T) = \frac{1}{kT} \int_{V_{\text{cell}}} \exp\left[-U/kT\right] \mathrm{d}V, \tag{13}$$

where V_{cell} is the free volume in cage j and U is the potential energy between the guest molecule i and the cage framework. These values are calculated during the MC process [24]. $C_{\text{large,THF}}$ is approximately six orders of magnitude larger than $C_{\text{large,H2}}$. $C_{\text{THF,small}}$ is close to zero due to the high positive potential energy. The fugacity of hydrogen can be obtained from the PVT relationship [25]. As THF is soluble in water, the fugacity of THF can

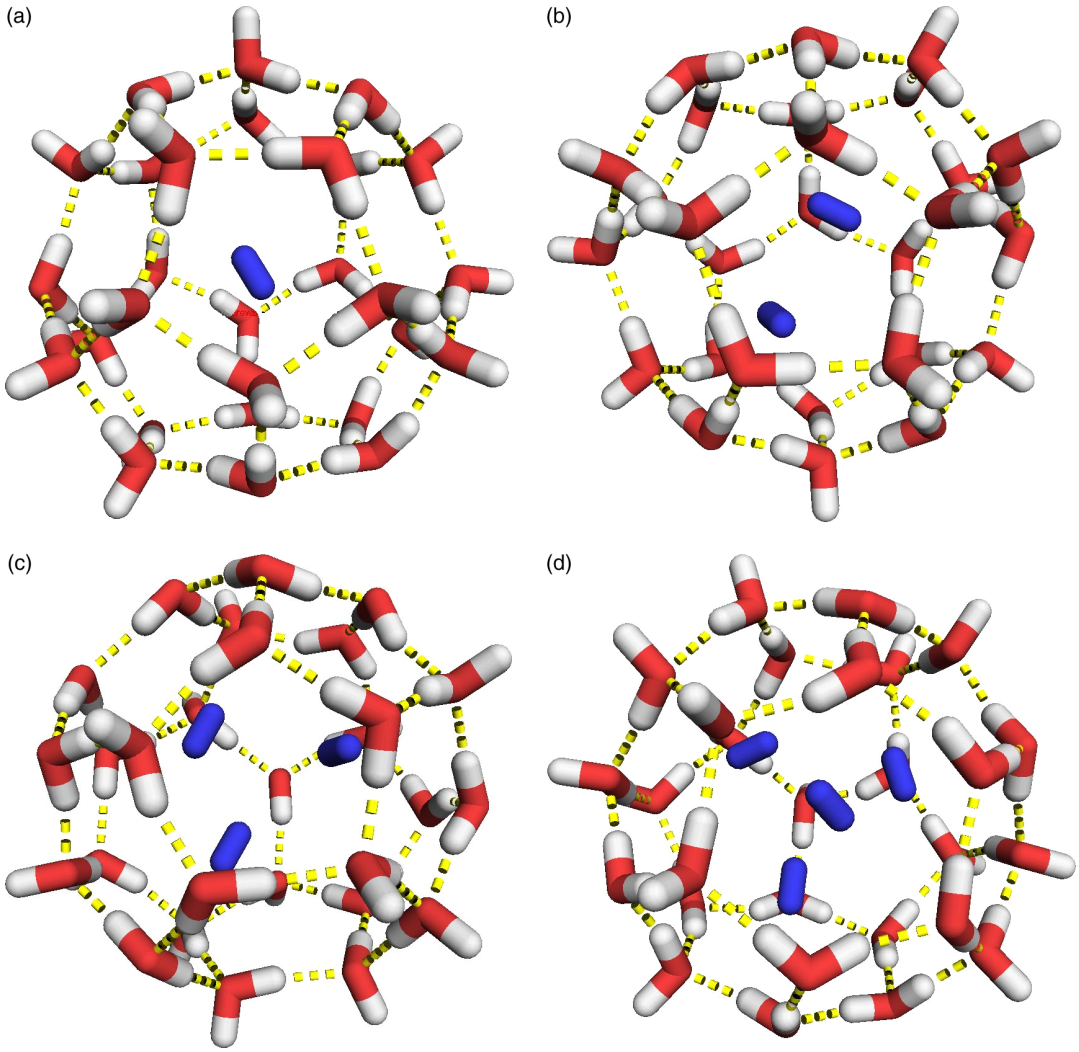

Figure 7. The configuration of hydrogen molecules in a large cage: (a) single occupancy of hydrogen in a large cage; (b) double occupancy of hydrogen in a large cage; (c) triple occupancy of hydrogen in a large cage; and (d) quadruple occupancy of hydrogen in a large cage.

be calculated by [25]

$$f_i = x_i \gamma_i \phi_i^{\mathrm{Sat}} P_i^{\mathrm{Sat}} \exp\left[\frac{1}{RT}\int_{P_i^{\mathrm{Sat}}}^{P} v_i \mathrm{d}P\right], \qquad (14)$$

where x_i is the composition of the aqueous liquid phase, γ_i is the activity coefficient, ϕ_i^{Sat} is the fugacity coefficient, P_i^{Sat} is the saturated pressure and v_i is the molar volume. The saturated pressure is calculated from the Korean thermo physical properties data bank equation [26], and the activity coefficients are calculated from a UNIQUAC model [27]. The results are shown in Figure 8. In addition, the single occupancy of hydrogen in small cages is compared with the result of Katsumasa et al. [19], which relates to the GCMC simulation of pure hydrogen hydrate at 273 K. The GCMC results show a similar tendency in terms of pressure dependence with the Langmuir isotherm for pressures ranging 0.1 to 200 MPa and with Katsumasa's simulation results for pressures ranging 100 to 200 MPa. The hydrogen storage capacity is plotted in Figure 9. The amount of hydrogen increases to 1.1 wt% as the pressure increases. The GCMC results were compared with the gas release experimental data [11], NMR [11] and Langmuir isotherm. The simulation results were found to be in good agreement with the NMR data.

Figures 10 and 11 show the specific occupancy and selectivity of guest molecules in large cages and small cages, respectively, as the pressure varies. In large cages, the occupancy of THF is decreased slightly and the multiple occupancy of hydrogen increases as the pressure increases. The large cages are capable of containing four

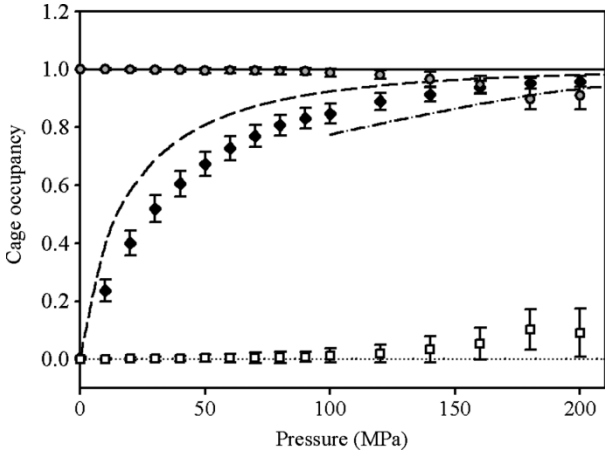

Figure 8. Occupancy of small cages (diamonds) and large cages (circles, THF; squares, hydrogen) obtained from the GCMC results. The results are compared with the Langmuir isotherm (dashed line, hydrogen in small cages; solid and dotted lines, respectively, THF and hydrogen in large cages) and Katsumasa's simulation results [19] (dashed-dotted line). The results of Katsumasa et al. denote single occupancy of a pure hydrogen hydrate in small cages at 273 K.

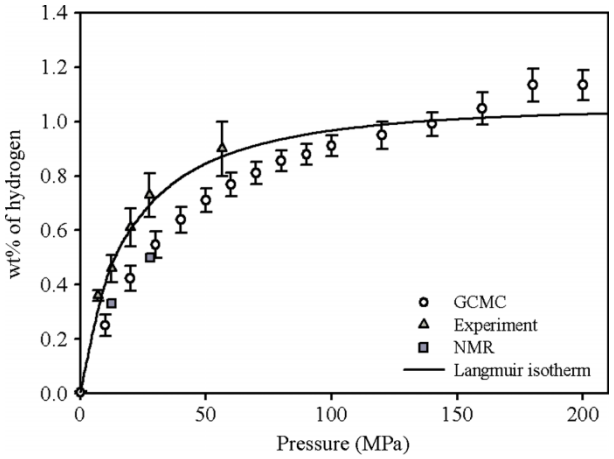

Figure 9. Hydrogen storage capacity in THF–H_2 hydrates: circles denote the results of GCMC; triangles denote the results of the gas release experiment [11]; squares denote the NMR data [11]; and the solid line denotes the Langmuir isotherm.

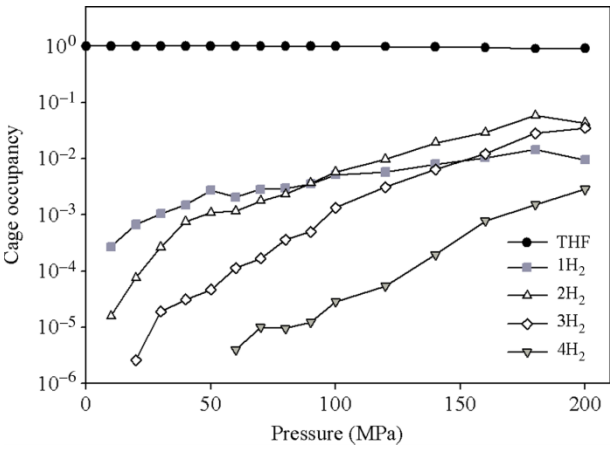

Figure 10. Occupancy and selectivity of guest molecules in large cages: circles denote THF; squares denote single hydrogen occupancy; triangles denote double hydrogen occupancy; diamonds denote triple hydrogen occupancy; and reverse triangles denote quadruple hydrogen occupancy.

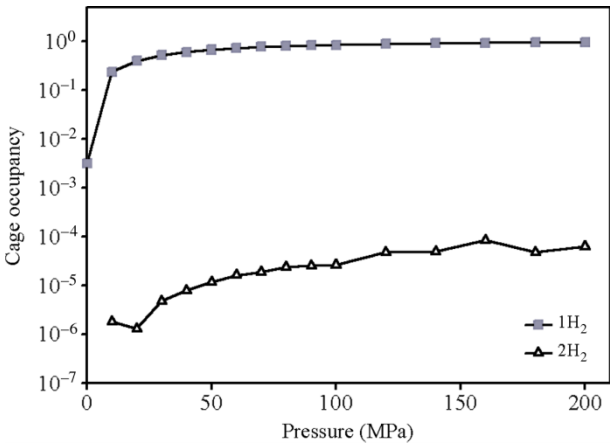

Figure 11. Occupancy in small cages: squares and triangles denote single and double hydrogen occupancy, respectively.

hydrogen molecules. However, most large cages select THF as a guest molecule, and hydrogen molecules only occupy approximately 10% among the large cages, even at 200 MPa. In small cages, the empty cages have a large portion at low pressures but most become filled with hydrogen as the pressure increases. Most small cages are filled with a single hydrogen molecule, and double occupancy is scarcely detected. Small cages select only hydrogen for guest molecules as THF molecules are too large to be encapsulated in small cages.

4. Conclusions

Binary THF–H_2 sII hydrates has been studied via GCMC simulation for various pressures. The equilibrium configuration obtained from GCMC provides information regarding the cage occupancy and selectivity of guest molecules in sII clathrate hydrates. The results of this study show that the dominant configuration in binary THF–H_2 hydrates is a single THF molecule in a large cage and a single hydrogen molecule in a small cage. Particularly, nearly all large cages have THF with a guest molecule at a pressure below 100 MPa. Multiple occupancy of hydrogen comprised a significant portion in large cages at the high pressure region above 100 MPa; however, binary hydrates are practically useless at extremely high pressures. Thus, it can be assumed that the hydrogen capacity in binary THF–H_2 sII hydrates is highly dependent on the molecules singly occupied in small cages.

Note

1. Email: cian75@kaist.ac.kr

References

[1] W.L. Mao, H. Mao, A.F. Goncharov, V.V. Struzhkin, Q. Guo, J. Hu, J. Shu, R.J. Hemley, M. Somayazulu, and Y. Zhao, *Hydrogen clusters in clathrate hydrate*, Science 27 (2002), pp. 2247–2249.

[2] M.H.F. Sluiter, R.V. Belosludov, A. Jain, V.R. Belosludov, H. Adachi, Y. Kawazoe, K. Higuchi, and T. Otani, Ab initio *study of hydrogen hydrate clathrates for hydrogen storage within the ITBL environment*, LNCS 2858 (2003), pp. 330–341.

[3] S. Patchkovskii and J.S. Tse, *Thermodynamic stability of hydrogen clathrates*, PNAS 100 (2003), pp. 14645–14650.

[4] W.L. Mao and H. Mao, *Hydrogen storage in molecular compounds*, PNAS 101 (2004), pp. 708–710.

[5] M.H.F. Sluiter, H. Adachi, R.V. Belosludov, V.R. Belosludov, and Y. Kawazoe, Ab initio *study of hydrogen storage in hydrogen hydrate clathrates*, Mater. Trans. 45 (2004), pp. 1452–1454.

[6] S. Alavi, J.A. Ripmeester, and D.D. Klug, *Molecular-dynamics study of structure II hydrogen clathrates*, J. Chem. Phys. 123 (2005), p. 024507.

[7] H. Lee, J. Lee, D.Y. Kim, J. Park, Y.T. Seo, H. Zeng, I.L. Moudrakovski, C.I. Ratcliffe, and J.A. Ripmeester, *Tuning clathrate hydrates for hydrogen storage*, Nature 434 (2005), pp. 743–746.

[8] S. Alavi, J.A. Ripmeester, and D.D. Klug, *Molecular-dynamics simulations of binary structure II hydrogen and tetrahydrofurane clathrates*, J. Chem. Phys. 124 (2006), p. 014704.

[9] S. Lee, P. Yedlapalli, and J.W. Lee, *Excess Gibbs potential model for multicomponent hydrogen clathrates*, J. Phys. Chem. B 110 (2006), pp. 26122–26128.

[10] K.C. Hester, T.A. Strobel, E.D. Sloan, C.A. Koh, A. Huq, and A.J. Schultz, *Molecular hydrogen occupancy in binary THF–H_2 clathrate hydrates by high resolution neutron diffraction*, J. Phys. Chem. B 110 (2006), pp. 14024–14027.

[11] I.A. Strobel, C.H. Taylor, K.C. Hester, S.F. Dec, C.A. Koh, K.T. Miller, and E.D. Sloan, Jr., *Molecular hydrogen storage in binary THF–H_2 clathrate hydrates*, J. Phys. Chem. B 110 (2006), pp. 17121–17125.

[12] T.C.W. Mak and R.K. McMullan, *Polyhedral clathrate hydrates. X. Structure of the double hydrate of tetrahydrofuran and hydrogen sulfide*, J. Chem. Phys. 42 (1965), pp. 2732–2737.

[13] H.J.C. Berendsen, J.R. Grigera, and T.P. Straatsma, *The missing term in effective pair potentials*, J. Phys. Chem. 91 (1987), pp. 6269–6271.

[14] A.E. Frisch, M.J. Frisch, and G.W. Trucks, *Gaussian 03 User's Reference*, Gaussian, Inc., Wallingford, CT, 2005.

[15] W.D. Cornell, P. Cieplak, C.L. Bayly, I.R. Gould, K.M. Merz, Jr., D.M. Ferguson, D.C. Spellmeyer, T. Fox, J.W. Caldwell, and P.A. Kollman, *A second generation force field for the simulation of proteins, nucleic acids, and organic molecules*, J. Am. Chem. Soc. 117 (1995), pp. 5179–5197.

[16] N.J. English, *Molecular dynamics simulations of liquid water using various long-range electrostatics techniques*, Mol. Phys. 103 (2005), pp. 1945–1960.

[17] M.P. Allen and D.J. Tildesley, *Computer Simulation of Liquids*, Oxford University Press, Oxford/New York, 1987.

[18] T.M. Reed and K.E. Gubbins, *Applied Statistical Mechanics*, McGraw-Hill, New York, 1973.

[19] K. Katsumasa, K. Koga, and H. Tanaka, *On the thermodynamic stability of hydrogen clathrate hydrates*, J. Chem. Phys. 127 (2007), p. 044509.

[20] S.R. Challa, D.S. Sholl, and J.K. Johnson, *Adsorption and separation of hydrogen isotopes in carbon nanotubes: Multicomponent grand canonical Monte Carlo simulations*, J. Chem. Phys. 116 (2002), pp. 814–824.

[21] V. Lachet, A. Boutin, B. Tavitian, and A.H. Fuchs, *Grand canonical Monte Carlo simulations of adsorption of mixtures of xylene molecules in faujasite zeolites*, Faraday Discuss. 106 (1997), pp. 307–323.

[22] P.J. Back and L.A. Woolf, *(p, V, T, x) measurements for tetrahydrofuran and {$xC_4H_8O + (1 - x)H_2O$}*, J. Chem. Thermodyn. 30 (1998), pp. 353–364.

[23] N.B. Vargaftik, *Tables on the Thermophysical Properties of Liquids and Gases*, John Wiley & Sons, Inc., New York, 1975.

[24] J.W. Tester, R.L. Bivins, and C.C. Herrick, *Use of Monte Carlo in calculating the thermodynamic properties of water clathrates*, AIChE J. 18 (1972), pp. 1220–1230.

[25] J.M. Smith and H.C. Van Ness, *Introduction to Chemical Engineering Thermodynamics*, McGraw-Hill, New York, 1987.

[26] C.S. Lee, K.P. Yoo, W.Y. Kim, and H. Lee, *Korea thermophysical properties data bank*, available at http://www.cheric.org/research/kdb/hcprop/showcoef-php?cmpid=1035

[27] J. Gmehling, U. Onken, and W. Arlt, *Vapor–liquid equilibrium data collection*, *Chemistry data series*, *vol 1*, *part 1a*, Dechema, Frankfurt, 1977.